catalysts

MDPI

Article

Electric Field Promoted Complete Oxidation of Benzene over $PdCe_xCo_y$ Catalysts at Low Temperature

Feixiang Shen [1,2], Ke Li [1], Dejun Xu [1], Xiaobo Li [3], Xuteng Zhao [1], Ting Chen [1], Reggie Zhan [1] and He Lin [1,*]

[1] The Key Laboratory for Power Machinery and Engineering of the Ministry of Education, Shanghai Jiao Tong University, Shanghai 200240, China; shenfeixiang@sjtu.edu.cn (F.S.); like123@sjtu.edu.cn (K.L.); xudejun@sjtu.edu.cn (D.X.); zhaoxuteng@sjtu.edu.cn (X.Z.); chenting@sjtu.edu.cn (T.C.); reggiezhan@sjtu.edu.cn (R.Z.)

[2] National Engineering Laboratory for Marine and Ocean Engineering Power System, Shanghai 200090, China

[3] Shanghai Marine Diesel Engine Research Institute, Shanghai 200090, China; lixiaobo19860213@163.com

* Correspondence: linhe@sjtu.edu.cn; Tel.: +86-21-3420-7774; Fax: +86-21-3420-5959

Received: 18 November 2019; Accepted: 13 December 2019; Published: 16 December 2019

Abstract: The application of electric field promotes benzene oxidation significantly over Pd/Co_xCe_y catalysts. For 1% Pd loading catalysts, the complete oxidation of benzene can be realized at 175 °C with an electric field under an input current of 3 mA, 79 °C lower than the temperature demanded for complete benzene conversion without electric field. The introduction of electric field can save Pd loading in the catalysts while maintaining high benzene conversion. The characterization experiments showed that CeO_2 reduction was accelerated with electric field and created more active oxygen, promoting the formation of active sites on the catalyst surface. The OH removal ability of PdO was enhanced by forming CoO(OH) species, which can easily dehydroxylate since the reduction of Co^{3+} was promoted by the electric field. The optimized Ce/Co ratio is a balance between oxygen availability and OH removal ability.

Keywords: low temperature benzene oxidation; electric field; oxygen availability; dehydroxylation process

1. Introduction

Nowadays, volatile organic compound (VOC) abatement has aroused wide concern due to its harmful effects on human health and the environment [1]. Exposure to VOCs can induce mutagenic and teratogenic effects on human body and cause cancer, cardiovascular, and other insusceptible diseases. Among various VOC removal methods, catalytic oxidation has been suggested as the most effective technique and has been extensively investigated for many decades [2–11]. Precious metal based catalysts such as Pd and Pt have be proved to be highly active for benzene oxidation. However, complete benzene conversion over the most effective catalysts that have been studied cannot be achieved below 200 °C [5,10–12] and a high loading of noble metal is demanded to further promote the catalytic activity, leading to increasing costs of catalysts. Thus, more effort should be focused on cutting down noble metal loading while maintaining high catalytic activity.

Recently, an electric field promoted catalytic system was reported by Y. Sekine' group [13–17], who proved that the electric field could highly improve the reaction at low temperature. In previous work [14,17,18], the electric field promoted system was applied on CH_4 oxidation over Pd/Ce_mZr_n and Pd/Co_3O_4 series catalysts, and ignition of CH_4 occurred at a temperature below 300 °C over catalysts with only 1% Pd loading, nearly 70 °C lower than the conventional reaction system. However, further

application of an electric field promoted system on other catalytic fields has not been reported. In this study, the electric field was applied to improve benzene oxidation over Pd based catalysts.

It is generally recognized that Ce oxides possess high oxygen storage capacity and can improve the metal dispersion [2,7,9,19–21]. Co addition in the support can increase the surface acidic sites and the dispersion of active components [22]. The interaction between Co and Ce showed a significant improvement in the reducibility of Co [21]. Co and Ce composite oxides have been used in many oxidation applications such as VOC and diesel soot combustion. In this paper, benzene was selected as the model VOC since it is one of the most abundant VOCs in the atmosphere. A series of x%Pd/Co$_m$Ce$_n$ catalysts were synthesized and applied in the electric field promoted catalytic system for benzene oxidation. The promoting effect of the electric field on catalytic activity was investigated with X-ray diffraction, X-ray photoelectron spectroscopy, H_2-temperature programed reduction and the Diffuse infrared spectroscopy technique.

2. Results

2.1. Benzene Oxidation Activity

As shown in Figure 1, The benzene conversion increased obviously with the input current and complete benzene oxidation could be realized below 200 °C over catalysts under 3 mA. However, there was no obvious promotion of catalytic activity as the input current rose from 3 mA to 4 mA. Thus, 3 mA was selected as the optimal current value considering the input power consumption. Figure 2 illustrates the benzene conversion over catalysts with different Ce/Co ratios and Pd loading. Without the application of the electric field, the impact of the Ce/Co ratio on catalytic activity was distinct in the order of Ce$_{0.5}$Co$_{0.5}$ > Ce$_{0.75}$Co$_{0.25}$ > Ce$_{0.25}$Co$_{0.75}$. However, catalysts with a Ce$_{0.25}$Co$_{0.75}$ oxide support exhibited the highest activity with a T_{90} of 175 °C under an electric current of 3 mA, demonstrating that the promoting effect of an electric field is highly dependent on the Ce/Co ratio. The performances of catalysts with different Pd doping percent are shown in Figure 2b. The T_{90} of the m% Pd/Co$_{0.75}$Ce$_{0.25}$ catalyst decreased as the Pd loading level increased, and the promotion effect of the electric current could compensate for the activity decline caused by an decrease in the Pd loading. The light off temperature over 1% Pd/Co$_{0.75}$Ce$_{0.25}$ under the electric current of 3 mA was 229 °C, lower than that of 233 °C over catalysts with a 2% Pd loading, suggesting that the introduction of an electric current can save Pd loading while maintaining a high level of catalytic activity. Table 1 illustrates the input current and voltage in the experiment. It can be found that the input voltage varied due to the change in electric assistance of the catalyst at different temperatures.

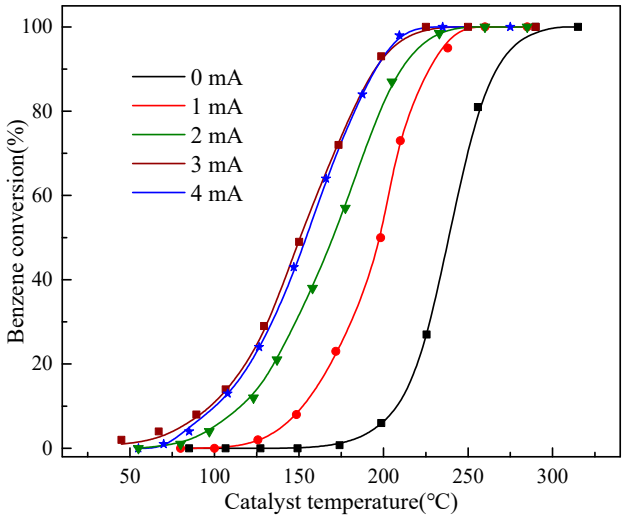

Figure 1. Benzene conversion efficiency over a 1% PdCe$_{0.25}$Co$_{0.75}$ catalyst at different input currents.

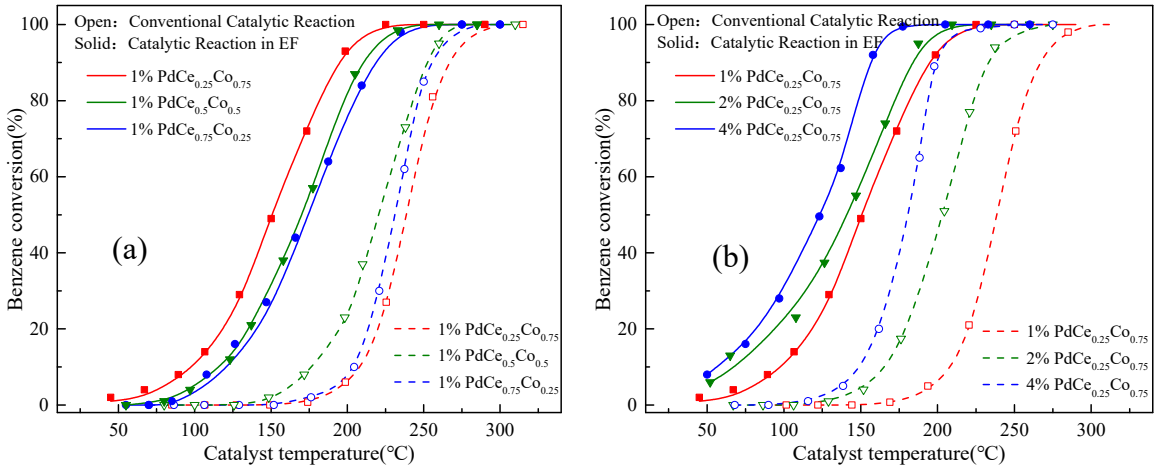

Figure 2. Benzene conversion efficiency over the m% $PdCe_xCo_y$ catalyst. EF: electric field, the input current is 3 mA. (**a**) catalysts with different Co/ratio; (**b**) catalysts with different Pd loading.

Table 1. Results of benzene oxidation over the m% $PdCe_xCo_y$ catalysts.

Sample	Current (mA)	Voltage (V)	T_{90}	T_{90} in EF	E_a	E_a in EF
1% $PdCe_{0.75}Co_{0.25}$	3	267–703	255	219	88.9	60.9
1% $PdCe_{0.5}Co_{0.5}$	3	237–678	252	200	99.8	58.7
1% $PdCe_{0.25}Co_{0.75}$	3	212–609	267	185	110.5	54.9
2% $PdCe_{0.25}Co_{0.75}$	3	165–528	233	173	78.2	50.8
4% $PdCe_{0.25}Co_{0.75}$	3	139–445	199	156	65.4	48.1

Figure 3 illustrates the Arrhenius plots on benzene oxidation for the tested samples. The E_a for the oxidation reaction was potentially reduced under an electric field. The E_a over the 1% $Pd/Co_{0.75}Ce_{0.25}$ catalyst was 54.9 kJ in the electric field, compared with 110.5 kJ in the reaction without an electric field. Pd loading lowered the E_a value in the conventional catalytic reaction, however, there was hardly any difference between the E_a values over catalysts with different Pd loading levels under 3 mA. This indicates that the enhancement of the electric current for benzene oxidation mainly occurred on the support of the catalyst.

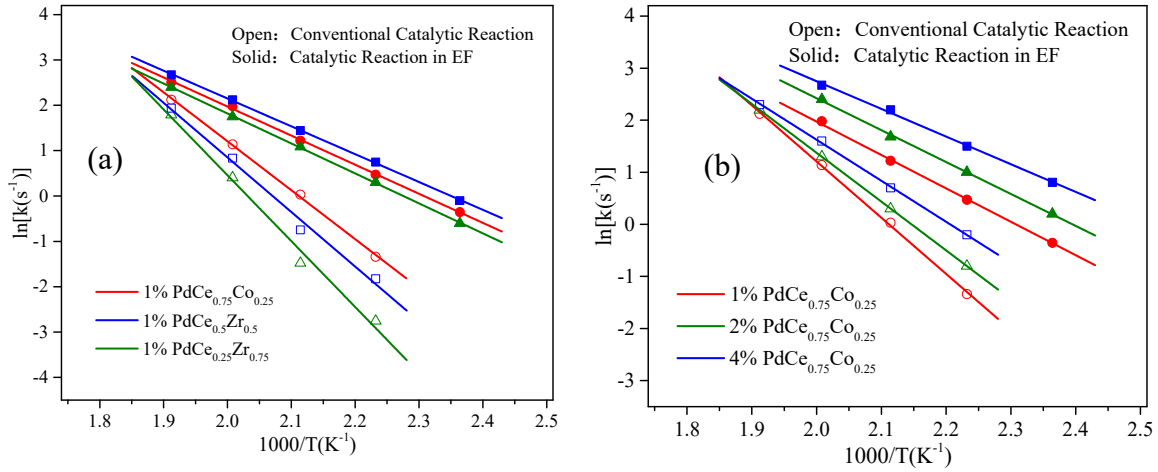

Figure 3. Arrhenius plots of benzene oxidation over the m% $PdCe_xCo_y$ catalyst. EF: electric field, the input current is 3 mA. (**a**) catalysts with different Co/ratio; (**b**) catalysts with different Pd loading.

2.2. Catalyst Characterization

Figure 4a shows the XRD patterns of fresh 1% $PdCe_xCo_y$ catalysts. The reflections located at 28.29°, 33.94°, 48.81°, 58.01°, 60.89°, and 76.71° corresponded to the planes of the CeO_2 fluorite structure, while the profile of Co_3O_4 showed peaks centered at 31.2°, 36.8°, 44.8°, 59.3°, and 65.2°. Diffraction peaks of CeO_2 weakened and shifted slightly to higher temperatures with the increase in the Co percent, indicating the part incorporation of Co species into the CeO_2 fluorite structure. No XRD patterns of Pd related species was observed in the figure, indicating a good Pd dispersion on the surface of the catalyst. The decrease in the average crystalline size with the rise in Co percent further proved the incorporation of Co ions into the CeO_2 fluorite lattice because the size of the coordinated Co^{2+} (0.82 Å) and Co^{3+} (0.65 Å) was lower than the Ce^{3+} or Ce^{4+} [23,24].

As shown in Figure 4b, CeO_2 related reflections in the XRD profiles of treated catalysts exhibited a shift to a lower degree. Compared with fresh catalysts, the lattice parameter and weak peak intensity of the treated catalysts were smaller, which may have been caused by Ce^{4+} reduction under an electric field. Diffraction reflections of Co_3O_4 hardly underwent any change under the electric field, suggesting that the reduction degree of Co_3O_4 is low when compared with CeO_2. However, since no Ce_2O_3 and CoO were detected in the XRD profiles, the reduction of CeO_2 and Co_3O_4 under an electric current needs to be further proven by the following experiment.

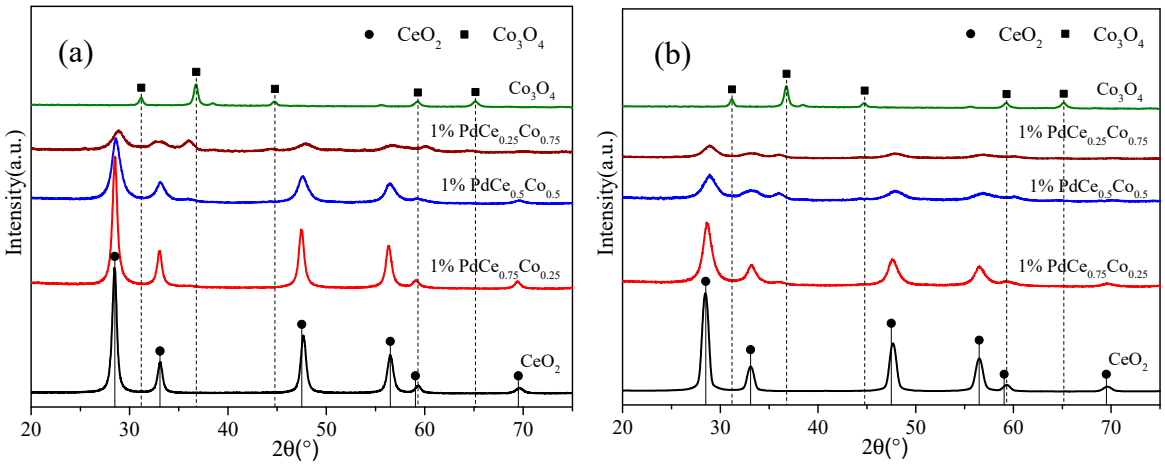

Figure 4. X-ray photoelectron spectroscopy results of (**a**) fresh and (**b**) treated 1% $PdCe_xCo_y$ samples (the input current is 3 mA).

The XPS results of Ce 3d are shown in Figure 5a. The spectra can be fitted with eight asymmetric peaks, and the peaks at 885.6 eV and 903.8 eV were ascribed to the Ce^{3+} species and others were related to the Ce^{4+} species [25,26]. It is widely accepted that Ce^{3+} can promote the formation of lattice oxygen defects and redox transformation between Ce^{3+} and Ce^{4+}, which are associated with catalytic activity at low temperature [18,27]. As shown in Table 2, the Ce^{3+} concentration increased with the Co/Ce ratio of the sample, indicating the reduction of Ce^{4+} by Co^{2+} incorporated in the lattice. However, the activity of the catalyst did not show the same trend, which may be due to the fact that the increase in the Co/Ce ratio led to a low absolute content of Ce species. After being treated under an electric field with the input current of 3 mA, the samples possessed a higher Ce^{3+} concentration on the surface, indicating the reduction of Ce^{4+} to Ce^{3+} with an electric current through the catalyst. The CeO_2 fluorite structure is a typical oxide semiconductor with oxygen ion conducting behaviors, and tends to undergo a valence decrease due to the access to electrons from the input current.

$$2CeO_2 + e^- \rightarrow Ce_2O_3 + O^- \quad (1)$$

The Co 2p spectra is composed of two peaks of Co $2p_{3/2}$ and Co $2p_{1/2}$ with a binding energy value at 780.3 and 796.1 eV, respectively. The asymmetric peaks in Co $2p_{3/2}$ ranging from 780.3 to 780.8 and 779.3 to 779.7 eV corresponded to the tetrahedral Co^{2+} and octahedral Co^{3+} in Co_3O_4. The satellite peak at 786.5 eV was ascribed to the octahedral Co^{2+} cation in Co_3O_4, indicating that the Co_3O_4 spinel was partially inverse. As shown in Table 3, For fresh samples, the ratios of $Co^{2+}/(Co^{2+} + Co^{3+})$ decreased with the rise in the Co/Ce ratio; in contrast to the trend of the $Ce^{3+}/(Ce^{4+} + Ce^{3+})$ ratio, indicating that the equation below may occur in the synthesis procedure.

$$Co^{2+} + Ce^{4+} \rightarrow Co^{3+} + Ce^{3+} \quad (2)$$

After being treated in the electric field, the $Co^{2+}/(Co^{2+} + Co^{3+})$ ratio increased and the treated 1% $PdCe_{0.5}Co_{0.5}$ showed the highest Co^{2+} content, which is a balance between Equations (2) and (3).

$$Co^{3+} + e^{-} \rightarrow Co^{2+} \quad (3)$$

The O 1s spectra can be divided into two main peaks, as shown in Figure 5c. The peak with a BE value in the range of 529.7–529.8 eV corresponded to the lattice oxygen (O_L), and the peak of the surface chemisorbed oxygen (O_A) was centered at 531.0–531.5 eV. The ratio of $O_A/(O_L + O_A)$ in fresh catalysts followed the order $Ce_{0.25}Co_{0.75} > Ce_{0.5}Co_{0.5} > Ce_{0.75}Co_{0.25}$, in the same trend of the $Ce^{3+}/(Ce^{4+} + Ce^{3+})$ ratio. This indicates that the Co incorporation in the lattice led to the weakening of Ce–O bonds, promoting the formation of O_A. Compared with the fresh catalysts, the treated sample showed an increase in the $O_A/(O_L + O_A)$ ratio and the sequence turned to $Ce_{0.25}Co_{0.75} < Ce_{0.5}Co_{0.5} < Ce_{0.75}Co_{0.25}$, indicating that the Ce species is more responsible for the formation of O_A due to the fact that the reduction of Ce^{4+} is quicker than that of the Co^{3+} reduction with an electric current through the catalysts. It can be concluded from the XPS results that CeO_2 and Co_3O_4 can easily be reduced by gaining electrons from the input electric current. Additionally, the quick reduction of CeO_2 can release more active oxygen species, which is beneficial for benzene oxidation.

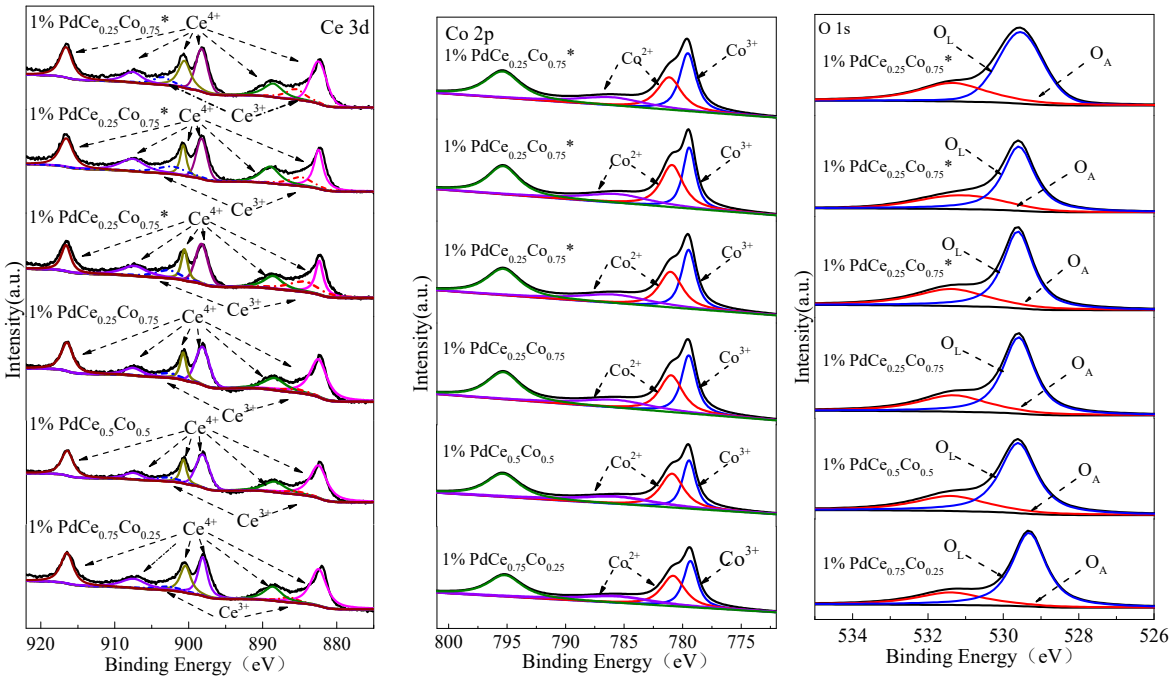

Figure 5. X-ray photoelectron spectroscopy spectra of the fresh and treated 1% $PdCe_xCo_y$ catalysts (termed as *m*% 1% $PdCe_xCo_y$ *, the input current is 3 mA). (**a**) Ce (3d); (**b**) Co (2p)' and (**c**) O (1s).

Table 2. Solid property of the tested 1% $PdCe_xCo_y$ samples.

Sample	Lattice Parameter (nm)		BET Area (m^2/g)		Crystallite Size from XRD (nm)	
	Fresh	Treated	Fresh	Treated	Fresh	Treated
1% $PdCe_{0.75}Co_{0.25}$	0.4420	0.4419	54.2	53.5	29.8	27.2
1% $PdCe_{0.5}Co_{0.5}$	0.5419	0.4413	55.3	55.3	27.3	25.3
1% $PdCe_{0.25}Co_{0.75}$	0.4419	0.4410	50.9	48.8	24.5	22.2

Table 3. Chemical states and structural properties of the 1% $PdCe_xCo_y$ catalysts.

Sample	Atomic Ratio of Ce^{3+} (%)		Atomic Ratio of Co^{2+} (%)		Atomic Ratio of O_A (%)		Lattice Parameter		Crystallite Size from TEM (nm)	
	Fresh	Treated	Fresh	Treated	Fresh	Treated	Fresh	Treated	Fresh	Treated
1% $PdCe_{0.75}Co_{0.25}$	7.8	17.4	50.3	55.4	19.2	32.8	4.821	4.819	29.8	27.7
1% $PdCe_{0.5}Co_{0.5}$	9.1	22.2	46.2	49.8	21.3	35.7	4.954	4.951	31.2	28.2
1% $PdCe_{0.25}Co_{0.75}$	11.6	28.5	43.3	44.4	23.5	40.7	4.987	4.983	33.6	29.2

2.3. H_2-Temperature Programed Reduction

H_2-TPR was conducted to study the reducibility of the 1% $PdCe_xCo_y$ catalysts. As Figure 6 shows, the α-peak centered at 312 °C was ascribed to the Co_3O_4 to CoO reduction and the β-peak at around 380 °C corresponded to the CoO to Co^0 reduction [28,29]. The peak μ and v centered at 421 °C and 629 °C were related to the reduction of $Ce^{4+} \rightarrow Ce^{3+}$ [30]. In the case without the electric field, the peak corresponding to the Pd^{2+} reduction was not obvious due to the low loading percentage of the Pd in the tested catalysts. The intensity of peak α corresponding to the Co^{3+} reduction increased with the rise in the Ce/Co ratio, indicating that more Co_3O_4 formed on the surface of the catalysts with high Ce content. The H_2 consumption of Ce^{4+} reduction did not increase linearly with Ce content, indicating that the oxygen in CeO_2 was indulged in the formation of Co_3O_4 and consumed at a lower temperature.

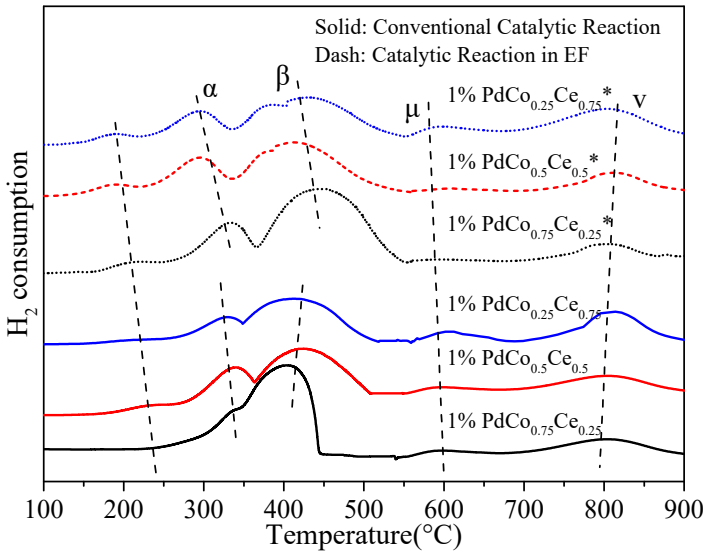

Figure 6. H_2-TPR spectra of Pd/Co_3O_4 without and with the electric field (termed as *m*% Pd/Co_3O_4 *, the input current is 3 mA).

In the case with an electric field, the peak intensity of Pd reduction increased significantly, indicating that more Pd with a high valence first formed with the electric current through the catalysts and then reduced by H_2. Since the H_2-TPR was conducted under no gaseous oxygen, the oxygen species from catalysts play an important role on the oxidation of Pd^0 and the formation of Pd^{2+}. The formation of Pd^{2+} will provide more active sites for benzene oxidation. The peak intensity of Co^{3+} reduction also increased under electric field while the reduction peak related to Ce^{4+} was weakened. It

can be concluded that the reduction of CeO_2 in the electric field provides active oxygen species for the formation of PdO_x species, which are highly active and provide sites for benzene adsorption and oxidation, leading to promoted catalytic activity at low temperature.

Figure 7 illustrates the in situ DRIFTS spectra of benzene oxidation at different temperatures. Without an electric current through the catalysts, the peak at 1155 cm^{-1} attributed to the O^{2-} bands of the absorbed gaseous O_2 was detected at 200 °C, and bands of the hydroxyl group (1633 cm^{-1}) and CO/CC (1598 and 1420 cm^{-1}) appeared at a temperature of 150 °C, suggesting that the oxidation of benzene was not by the oxygen species formed by gaseous O_2 in the catalytic oxidation process. This demonstrates that the benzene oxidation may obey the MvK mechanism rather than the E–R mechanism at temperatures below 200 °C. It is hard to tell which mechanism dominates the oxidation process at higher temperatures. The OH group vanished at 250 °C due to quick oxidation to H_2O. Bands of CO/CC species decreased with the temperature, giving rise to the band intensity of carbonate species (1360 and 1240 cm^{-1}) and CO_2 (2360 cm^{-1}). With an electric current through the catalysts, weak bands of CO/CC species at 1557 and 1430 cm^{-1} were detected only at 100 °C and 150 °C, while carbonates (1369 and 1238 cm^{-1}) and CO_2 (2350 cm^{-1}) related bands with a higher intensity were detected at the same temperature. This indicates the accelerated oxidation of benzene species in the electric field. Bands of OH group were not detected, which may be due to quick conversion under an electric field. No obvious changes were observed over the O^{2-} bands (1158 cm^{-1}), which emerged at the temperature above 200 °C, indicating that O^{2-} formed by gaseous oxygen may not be involved in benzene oxidation at a lower temperature. In other words, oxygen species from the bulk lattice may be highly involved in benzene oxidation with electric field at low temperature.

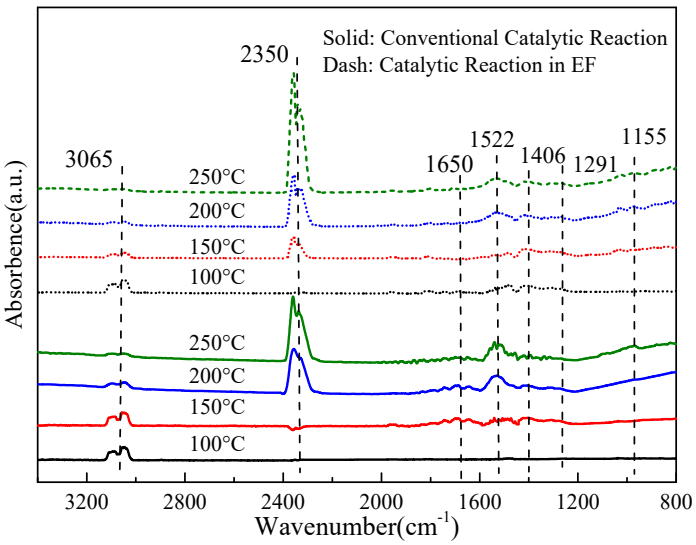

Figure 7. In situ Diffuse infrared spectroscopy results of benzene oxidation over 1% $PdCe_{0.5}Co_{0.5}$ catalyst. EF: electric field, the input current is 3 mA.

3. Discussion

The mechanism on benzene oxidation over Pd-based catalysts has been investigated intensely for the last few decades [5,10,12,21]. The rate determining step in benzene combustion at low temperature is the activation of the C–H bond over the PdO phase [31]. In the E–R reaction model, gaseous oxygen species will first adsorb on the active sites and then get involved in benzene oxidation. Furthermore, in the E–R reaction model, the benzene was mainly oxidized by oxygen species from the bulk catalyst. According to the Fourier Transform Infrared Spectrometer results, the oxidation of benzene obeys the MvK mechanism and the availability of oxygen from the bulk catalyst plays an important role in benzene oxidation. When an electric field was introduced, more active oxygen species were formed from the CeO_2 reduction, making the formation of more [PdO_x] sites, thus promoting the benzene

catalytic oxidation at low temperature. Since the catalyst under 3 mA exhibited the highest performance, this indicated that most oxygen species can be released from the CeO_2 lattice at the input current of 3 mA, and a further increase of input current cannot create more active species on the catalyst surface. When the temperature rises to higher than 200 °C, the adsorption of gaseous oxygen occurs and maybe both the MvK and E–R model dominate the benzene oxidation process.

Furthermore, the activity of Pd sites can be inhibited by the adsorption of water molecules and formation of less active PdOOH [31,32], resulting in the weakness of the catalyst performance. It was reported that CoO can facilitate the refresh of Pd sites by obtaining OH from the PdOOH species and formed CoOOH. However, the further dehydroxylation of CoOOH is a slow process. The FTIR experiment showed that the hydroxyl group species were not detected with an electric current through the catalysts, indicating that the removal of the hydroxyl group on the catalyst surface by transfer to the cobalt spinel was significantly accelerated, which may be another important factor leading to the promotion of benzene oxidation with an electric field. The quick removal of the OH group with an electric current through the catalysts can be attributed to the accelerated conversion of CoOOH to CoO due to the enhanced reducibility of Co^{3+} with an electric field, which has been demonstrated by the XPS results.

Based on the discussion above, the reduction of CeO_2 with an electric current through the catalysts provide active oxygen species and these oxygen species with high mobility form active sites around Pd species for benzene oxidation. The reduction of Co will facilitate the removal of OH species and promote the regeneration of PdO active sites. The Ce species and Co species in the catalyst is responsible for the formation of active sites (valued as oxygen availability) and the removal of the OH group (valued as OH removal ability) under an electric current. As shown in Figure 8, the Co/Ce ratio of the catalyst with the highest activity is a balance between these two effects.

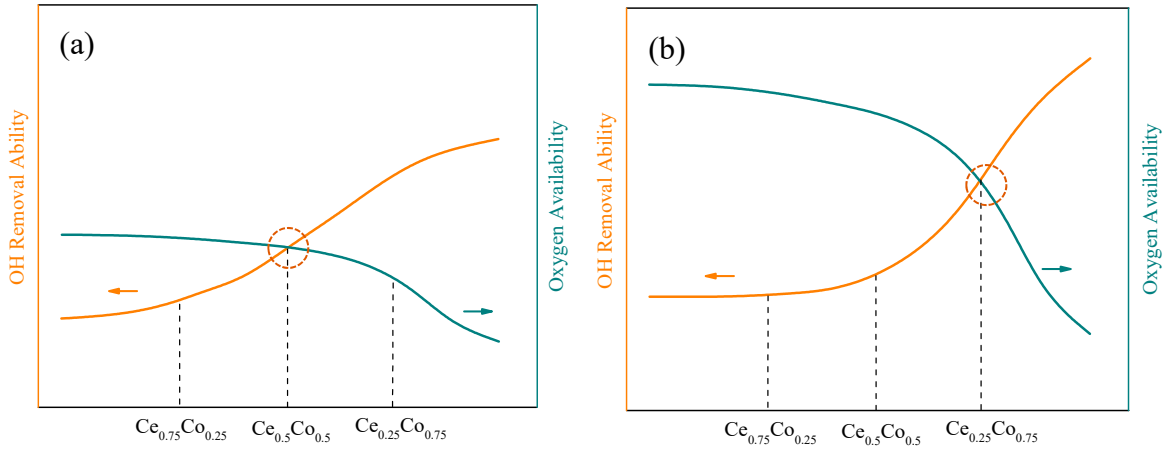

Figure 8. Balance between the oxygen availability and OH removal ability over the 1% $PdCe_xCo_y$ catalysts. (**a**) Without electric field; (**b**) With electric field.

4. Experimental

4.1. Catalyst Synthesis

The Pd/Co_xCe_y catalysts were synthesized by the self-propagating combustion method [33]. Palladium acetate ($Pd(OAc)_2$) was first dissolved in xylene and then the mixture was blended with a $Co(NO_3)_2{\cdot}6H_2O$ and $Ce(NO_3)_3{\cdot}6H_2O$ aqueous solution. Glycine (CH_2NH_2COOH) was poured into the mixture to neutralize nitrates. The solution was then poured into a corundum crucible in a muffle furnace and the temperature was set to 400 °C. After 4.5 h, the residue was collected and sieved to 40–60 meshes. The synthesized catalysts were identified as x% $PdCo_mCe_n$, where x is the mass percent of Pd, and m and n represent the mole ratio of the Co and Ce elements.

4.2. Catalytic Evaluation Method

The performance of the catalyst for benzene oxidation was evaluated in a cylindrical flow reactor. As shown in Figure 9, the electric field was generated by a direct current (DC) power supply and applied on the catalyst bed with platinum wire as the electrodes. The DC power supply was set to constant current output mode. The input current can be set to constant and the voltage is dependent on the resistance of the catalysts at different reaction temperatures. A gas mixture of 0.1%C_6H_6/10% O_2/90% N_2 was introduced into the reactor with a volumetric flow rate of 150 mL/min, corresponding to a gas space velocity of 60,000 h^{-1}. The concentrations of benzene were recorded with gas chromatography and a Thermo Nicolet IS10 FTIR spectrometer.

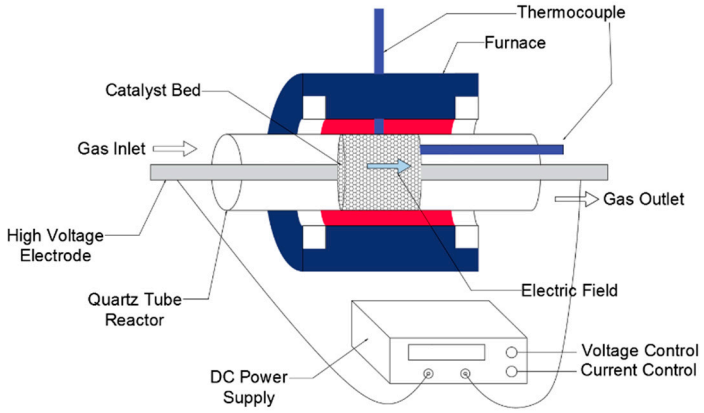

Figure 9. Experimental setup of the catalytic process combined with an electric field.

4.3. Catalyst Characterization

The N_2 sorption experiment was performed at −196 °C using a Quantachrome NOVA 2000e Automated Gas Sorption Instrument. The structure patterns of the catalysts were collected using a computerized Rigaku D/max-2200/PC x-ray diffractometer (XRD) equipped with Ni-filtered Cu Kα (k = 0.1528) radiation. The surface elemental composition of the catalysts were analyzed with an x-ray photoelectron spectroscopy (XPS). H_2 temperature programing reduction (TPR) tests were performed on Micrometrics Chemisorb 2720 equipment. Before the test, the catalysts were pretreated in N_2 at 450 °C for 1 h. The sample was then heated up from 20 °C to 800 °C at 10 °C/min in an atmosphere of 5% H_2, balanced with N_2. The water vapor from the reduction of Pd and Co_3O_4 was removed by a cold trap between the detector and the cell. The in situ DRIFTS test was performed by a FTIR spectrometer (Thermo IS 10). Before the test, the catalysts were treated in a N_2 atmosphere at 450 °C for 2 h. The spectra were recorded in a range from 4000 to 800 cm^{-1} at a spectra resolution of 1 cm^{-1}.

5. Conclusions

Electric field promoted catalytic system realizes the low temperature catalytic oxidation of benzene over 1% $PdCe_mCo_n$ catalysts. The 1% $PdCe_{0.5}Co_{0.5}$ exhibited the highest activity with the complete conversion of benzene at 185 °C under the electric current of 3 mA. Nearly half the Pd loading can be saved to achieve a high conversion level with an electric current through the catalysts. The characterization results showed that an electric field can enhance the oxygen mobility through facilitating the reduction of CeO_2, providing more active sites for benzene oxidation. Inhibition of the produced water molecules on the catalyst activity was eliminated due to the promoted "H_2O sink" effect of the Co_3O_4 support with an electric current through the catalysts. This research provides a novel catalytic technology for promoting the catalytic activities of catalysts with low Pd loading for benzene abatement.

Author Contributions: Conceptualization, F.S.; methodology, F.S. and K.L.; validation, D.X. and X.L.; formal analysis, X.Z., T.C. and R.Z.; investigation, H.L.; writing—original draft preparation, F.S. and K.L.

Funding: This research received no extra funding.

Acknowledgments: The author acknowledges financial support from the National Natural Science Foundation of China (51676127).

Conflicts of Interest: The authors declare no conflict of interest.

References

1. Li, W.B.; Wang, J.X.; Gong, H. Catalytic combustion of VOCs on non-noble metal catalysts. *Catal. Today* **2009**, *148*, 81–87. [CrossRef]
2. Cuo, Z.; Deng, Y.; Li, W.; Peng, S.; Zhao, F.; Liu, H.; Chen, Y. Monolithic Mn/Ce-based catalyst of fibrous ceramic membrane for complete oxidation of benzene. *Appl. Surf. Sci.* **2018**, *456*, 594–601. [CrossRef]
3. Ilieva, L.; Petrova, P.; Tabakova, T.; Zanella, R.; Abrashev, M.V.; Sobczak, J.W.; Lisowski, W.; Kaszkur, Z.; Andreeva, D. Relationship between structural properties and activity in complete benzene oxidation over Au/CeO_2–CoO_x catalysts. *Catal. Today* **2012**, *187*, 30–38. [CrossRef]
4. Ilieva, L.; Petrova, P.; Tabakova, T.; Zanella, R.; Kaszkur, Z. Gold catalysts on ceria doped with MeOx (Me = Fe, Mn, Co and Sn) for complete benzene oxidation: Effect of composition and structure of the mixed supports. *React. Kinet. Mech. Catal.* **2012**, *105*, 23–37. [CrossRef]
5. Kim, H.S.; Kim, T.W.; Koh, H.L.; Lee, S.H.; Min, B.R. Complete benzene oxidation over Pt-Pd bimetal catalyst supported on γ-alumina: Influence of Pt-Pd ratio on the catalytic activity. *Appl. Catal. A Gen.* **2005**, *280*, 125–131. [CrossRef]
6. Lin, S.S.Y.; Kim, D.H.; Ha, S.Y. Hydrogen Production from Ethanol Steam Reforming Over Supported Cobalt Catalysts. *Catal. Lett.* **2008**, *122*, 295–301. [CrossRef]
7. Mo, S.; Li, S.; Li, J.; peng, S.; Chen, J.; Chen, Y. Promotional effects of Ce on the activity of MnAl oxide catalysts derived from hydrotalcites for low temperature benzene oxidation. *Catal. Commun.* **2016**, *87*, 102–105. [CrossRef]
8. Petrova, P.; Tabakova, T.; Munteanu, G.; Zanella, R.; Tsvetkov, M.; Ilieva, L. Gold catalysts on Co-doped ceria for complete benzene oxidation: Relationship between reducibility and catalytic activity. *Catal. Commun.* **2013**, *36*, 84–88. [CrossRef]
9. Urbutis, A.; Kitrys, S. Dual function adsorbent-catalyst CuO-CeO_2/NaX for temperature swing oxidation of benzene, toluene and xylene. *Cent. Eur. J. Chem.* **2014**, *12*, 492–501. [CrossRef]
10. Tang, W.; Deng, Y.; Chen, Y. Promoting effect of acid treatment on Pd-Ni/SBA-15 catalyst for complete oxidation of gaseous benzene. *Catal. Commun.* **2017**, *89*, 86–90. [CrossRef]
11. Zuo, S.; Du, Y.; Liu, F.; Han, D.; Qi, C. Influence of ceria promoter on shell-powder-supported Pd catalyst for the complete oxidation of benzene. *Appl. Catal. A Gen.* **2013**, *451*, 65–70. [CrossRef]
12. He, C.; Li, J.; Li, P.; Cheng, J.; Hao, Z.; Xu, Z.-P. Comprehensive investigation of Pd/ZSM-5/MCM-48 composite catalysts with enhanced activity and stability for benzene oxidation. *Appl. Catal. B Environ.* **2010**, *96*, 466–475. [CrossRef]
13. Okada, S.; Manabe, R.; Inagaki, R.; Ogo, S.; Sekine, Y. Methane dissociative adsorption in catalytic steam reforming of methane over Pd/CeO_2 in an electric field. *Catal. Today* **2018**, *307*, 272–276. [CrossRef]
14. Li, K.; Liu, K.; Xu, D.J.; Ni, H.; Shen, F.X.; Chen, T.; Guan, B.; Zhan, R.; Huang, Z.; Lin, H. Lean methane oxidation over Co_3O_4/$Ce_{0.75}Zr_{0.25}$ catalysts at low-temperature: Synergetic effect of catalysis and electric field. *Chem. Eng. J.* **2019**, *369*, 660–671. [CrossRef]
15. Yabe, T.; Mitarai, K.; Kazumasa, O.; Ogo, S.; Sekine, Y. Low-temperature dry reforming of methane to produce syngas in an electric field over La-doped Ni/ZrO_2 catalysts. *Fuel Process. Technol.* **2017**, *158*, 96–103. [CrossRef]
16. Oshima, K.; Shinagawa, T.; Haraguchi, M.; Sekine, Y. Low temperature hydrogen production by catalytic steam reforming of methane in an electric field. *Int. J. Hydrog. Energy* **2013**, *38*, 3003–3011. [CrossRef]
17. Li, K.; Xu, D.; Liu, K.; Ni, H.; Shen, F.; Chen, T.; Guan, B.; Zhan, R.; Huang, Z.; Lin, H. Catalytic Combustion of Lean Methane Assisted by an Electric Field over Mn_xCo_y Catalysts at Low Temperature. *J. Phys. Chem. C* **2019**, *123*, 10377–10388. [CrossRef]

18. Li, K.; Liu, K.; Ni, H.; Guan, B.; Zhan, R.; Huang, Z.; Lin, H. Electric field promoted ultra-lean methane oxidation over Pd-Ce-Zr catalysts at low temperature. *Mol. Catal.* **2018**, *459*, 78–88. [CrossRef]
19. Karolewska, M.; Truszkiewicz, E.; Mierzwa, B.; Kępiński, L.; Raróg-Pilecka, W. Ammonia synthesis over cobalt catalysts doped with cerium and barium. Effect of the ceria loading. *Appl. Catal. A Gen.* **2012**, *445–446*, 280–286. [CrossRef]
20. Zuo, S.; Liu, F.; Tong, J.; Qi, C. Complete oxidation of benzene with cobalt oxide and ceria using the mesoporous support SBA-16. *Appl. Catal. A Gen.* **2013**, *467*, 1–6. [CrossRef]
21. Zuo, S.; Qi, C. Modification of Co/Al_2O_3 with Pd and Ce and their effects on benzene oxidation. *Catal. Commun.* **2011**, *15*, 74–77. [CrossRef]
22. Zhang, X.; Yuezong, C.; Zhuofeng, L.; Xuerong, Z.; He, G. Cobalt modification for improving potassium resistance of Mn/Ce-ZrO_2 in selective catalytic reduction. *Chem. Eng. Technol.* **2016**, *39*, 874–882.
23. Giménez-Mañogil, J.; Bueno-López, A.; García-García, A. Preparation, characterisation and testing of $CuO/Ce_{0.8}Zr_{0.2}O_2$ catalysts for NO oxidation to NO_2 and mild temperature diesel soot combustion. *Appl. Catal. B Environ.* **2014**, *152–153*, 99–107. [CrossRef]
24. Qin, R.; Chen, J.; Gao, X.; Zhu, X.; Yu, X.; Cen, K. Catalytic oxidation of acetone over $CuCeO_x$ nanofibers prepared by electrospinning method. *RSC Adv.* **2014**, 4. [CrossRef]
25. Aranda, A.; Agouram, S.; López, J.M.; Mastral, A.M.; Sellick, D.R.; Solsona, B.; Taylor, S.H.; García, T. Oxygen defects: The key parameter controlling the activity and selectivity of mesoporous copper-doped ceria for the total oxidation of naphthalene. *Appl. Catal. B Environ.* **2012**, *127*, 77–88. [CrossRef]
26. Martínez-Arias, A.; Hungría, A.B.; Munuera, G.; Gamarra, D. Preferential oxidation of CO in rich H_2 over CuO/CeO_2: Details of selectivity and deactivation under the reactant stream. *Appl. Catal. B Environ.* **2006**, *65*, 207–216. [CrossRef]
27. Luo, J.-Y.; Meng, M.; Li, X.; Li, X.-G.; Zha, Y.-Q.; Hu, T.-D.; Xie, Y.-N.; Zhang, J. Mesoporous Co_3O_4–CeO_2 and Pd/Co_3O_4–CeO_2 catalysts: Synthesis, characterization and mechanistic study of their catalytic properties for low-temperature CO oxidation. *J. Catal.* **2008**, *254*, 310–324. [CrossRef]
28. Liotta, L.; Di Carlo, G.; Pantaleo, G.; Deganello, G. Co_3O_4/CeO_2 and Co_3O_4/CeO_2–ZrO_2 composite catalysts for methane combustion: Correlation between morphology reduction properties and catalytic activity. *Catal. Commun.* **2005**, *6*, 329–336. [CrossRef]
29. Liotta, L.; Di Carlo, G.; Pantaleo, G.; Venezia, A.M.; Deganello, G. Co_3O_4/CeO_2 composite oxides for methane emissions abatement: Relationship between Co_3O_4–CeO_2 interaction and catalytic activity. *Appl. Catal. B* **2006**, *66*, 217–227. [CrossRef]
30. Liu, J.; Zhao, Z.; Wang, J.; Xu, C.; Duan, A.; Jiang, G.; Yang, Q. The highly active catalysts of nanometric CeO_2-supported cobalt oxides for soot combustion. *Appl. Catalb.* **2008**, *84*, 185–195. [CrossRef]
31. Ercolino, G.; Stelmachowski, P.; Grzybek, G.; Kotarba, A.; Specchia, S. Optimization of Pd catalysts supported on Co_3O_4 for low-temperature lean combustion of residual methane. *Appl. Catalb.* **2017**, *206*, 712–725. [CrossRef]
32. Zhang, F.; Hakanoglu, C.; Hinojosa, J.A.; Weaver, J.F. Inhibition of methane adsorption on PdO(101) by water and molecular oxygen. *Surf. Sci.* **2013**, *617*, 249–255. [CrossRef]
33. Guan, B.; Lin, H.; Zhu, L.; Huang, Z. Selective Catalytic Reduction of NO_x with NH_3 over Mn, Ce Substitution $Ti_{0.9}V_{0.1}O_{2-\delta}$ Nanocomposites Catalysts Prepared by Self-Propagating High-Temperature Synthesis Method. *J. Phys. Chem. C* **2011**, *115*, 12850–12863. [CrossRef]